



**HAL**  
open science

## Thermal Management of the Hexafly-Int Hypersonic Glider

Jean-Yves Andro, Roberto Scigliano, Alexander Kallenbach, Johan Steelant

► **To cite this version:**

Jean-Yves Andro, Roberto Scigliano, Alexander Kallenbach, Johan Steelant. Thermal Management of the Hexafly-Int Hypersonic Glider. HISST 2018, Nov 2018, MOSCOU, Russia. hal-01977955

**HAL Id: hal-01977955**

**<https://hal.science/hal-01977955v1>**

Submitted on 11 Jan 2019

**HAL** is a multi-disciplinary open access archive for the deposit and dissemination of scientific research documents, whether they are published or not. The documents may come from teaching and research institutions in France or abroad, or from public or private research centers.

L'archive ouverte pluridisciplinaire **HAL**, est destinée au dépôt et à la diffusion de documents scientifiques de niveau recherche, publiés ou non, émanant des établissements d'enseignement et de recherche français ou étrangers, des laboratoires publics ou privés.



## **Thermal Management of the Hexafly-Int Hypersonic Glider**

*Jean-Yves Andro<sup>1</sup>, Roberto Scigliano<sup>2</sup>, Alexander Kallenbach<sup>3</sup>, Johan Steelant<sup>4</sup>*

### **Abstract**

This paper presents the sizing and choice of the technological solutions used for the thermal management of the critical hot parts, the main structure and the equipment of the Hexafly-Int hypersonic glider. Air conditioning into the fairing is used during pre-flight operations so as to maintain the temperature of the vehicle with its equipment below 20°C. During the flight, the thermal integrity of the nose is based on a heat sink approach by using massive blocks of metallic materials coated by zirconium whereas the wing leading edges and the flaps are made in C/C-SiC material. Among different assessed solutions, the temperature of the main titanium structure is maintained below 700°C thanks to an extra high emissivity painting applied on its external face. Equipment is protected from radiative heat transfer of the main structure thanks to a light flexible microporous insulator named Aeroguard® which exhibits extra high insulation performance at low pressure into the stratosphere. This internal thermal protection system is kept in place on the internal faces of the main structure thanks to thin flexible wires which allow fast depressurization of the insulator and mechanical strength to vibrations during the ascent phase of the flight. All equipment is also protected from conductive heat transfer coming from the hot main structure by using low thermal conductivity fixations based on Vespel® material. A special thermal management is dedicated to telemetry electronic boxes so as to absorb their dissipated power into a heat sink based on phase changing material.

**Keywords:** *Thermal management, Thermal Protection system (TPS), Thermal Control System (TCS)*

### **Nomenclature**

C/C-SiC	Carbon fiber in Carbon Matrix covered with SiC
CFD	Computational Fluid Dynamics
EFTV	Experimental Flight Test Vehicle
ESM	Experimental Service Module
FEM	Finite Elements Method
PCM	Phase Changing Material
TCS	Thermal Control System
TPS	Thermal Protection System

---

<sup>1</sup> ONERA (French Aerospace Research Center), Information Processing and Systems Department, Design & Assessment of Aerospace Vehicles Unit, Chemin de la Hunière - BP 80100, FR-91123 Palaiseau Cedex, France, [jean-yves.andro@onera.fr](mailto:jean-yves.andro@onera.fr)

<sup>2</sup> CIRA scpa (Italian Aerospace Research Center), Structures and Materials Department, Thermo-structures and thermal control technologies and design lab. Via Maiorise snc, 81043 Capua (CE), Italy, [r.scigliano@cira.it](mailto:r.scigliano@cira.it).

<sup>3</sup> DLR-MORABA (German Aerospace Center - Mobile Rocket Base), Oberpfaffenhofen, 82234 Wessling, Germany, [Alexander.Kallenbach@dlr.de](mailto:Alexander.Kallenbach@dlr.de)

<sup>4</sup> ESA-ESTEC, Flight Vehicle and Aerothermodynamics Engineering Section TEC-MPA, P.O. Box 299, Noordwijk, Netherlands, [Johan.Steelant@esa.int](mailto:Johan.Steelant@esa.int)

## 1. Introduction

The HEXAFLY-INT vehicle, a 3 m long hypersonic glider, will be launched on top of a single stage sounding rocket up to an altitude of nearly 90 km. After the apogee, the vehicle will perform a first part of the descent trajectory aided by an Experimental Service Module (ESM), then after the separation it will perform a pull-out maneuver, to finally starting a gliding phase at Mach 8 at an altitude of nearly 30 000 m during few hundreds of seconds.

The glider aeroshape design makes maximum use of databases, expertise, technologies and materials elaborated in previously European community co-funded projects LAPCAT I & II [1][2], ATLLAS I & II [3][4] and HEXAFLY [5].

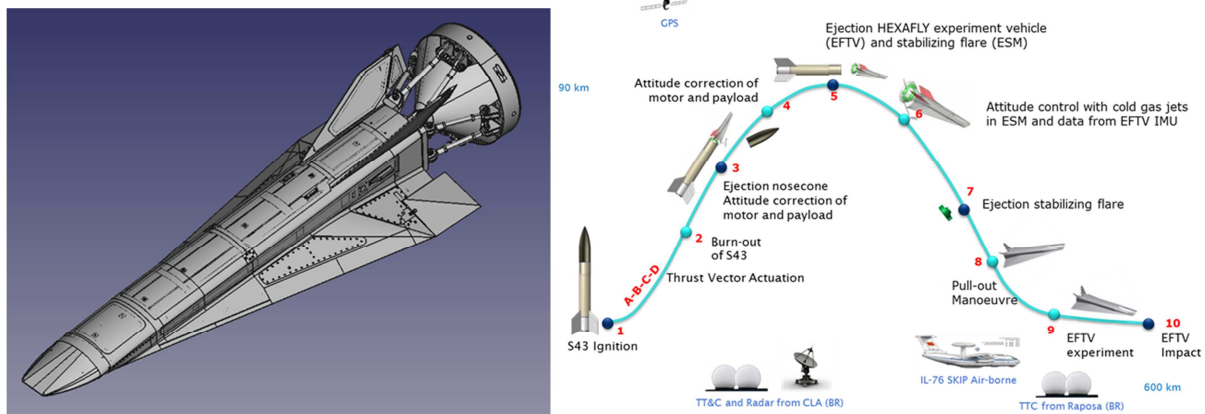


**Fig 1.** Hexafly-Int experimental flight test vehicle and profile mission

The whole mission is decomposed of two phases:

- Pre-flight operations where the equipment are switched on before the ignition of the booster. Some ground departed active cooling could be used during this phase.
- Flight where only passive solutions are scheduled due to the low cost approach of the project

## 2. Pre-flight operations

The HEXAFLY-Int vehicle is planned to be launched from the Alcântara Launch Center (CLA), Brazil at the top of a vertical booster under a fairing. For the installation phase, the vehicle is covered by an Integration Tower, which will be removed twice during pre-flight operations, first early in the countdown for about 100 min to perform RF tests and second for about 60 min prior to the launch.

So as to prevent heating from the sun during pre-flight operations, it is intended to utilize an existing cooling system established by CLA. The cooling based on an air conditioning system is designed to maintain the payload in a temperature range of 14 – 20°C. For the HEXAFLY-Int mission, the cooling ducts have to be adapted to allow the inflow of cold air to the backwards open hoods of the fairing. Alternatively, a Styrofoam cover could be built around the fairing and inflated by cold air. The two options are schematically shown in Fig 2.

This cooling system will maintain the structure of the experimental flight test vehicle below 20°C during all pre-flight operations. So, it will prevent also any radiative, conductive or free convective heating of the internal equipment even if they can still heat up from their own dissipated power during their stand-by mode prior to the lift-off of the booster.

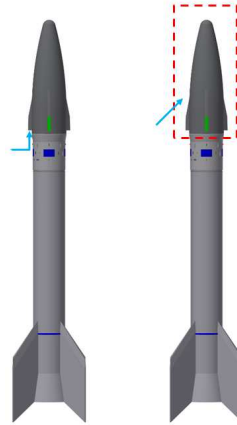


**Fig 2.** Hexafly-Int pre-flight cooling system options:  
 Left: Direct inflation of fairing - Right: Inflation of Styrofoam cover around fairing

### 3. Structure of the vehicle during flight

#### 3.1. Preliminary nodal simulations

As a low cost demonstrator, the main structure of Hexafly-Int vehicle is almost metallic. The chosen material is a Russian variant of titanium alloy, named BT-20, which is able to withstand 700°C along the reference trajectory.

ONERA performed 1D nodal thermal simulations of the 3 mm thick titanium panels of the structure to determine the best solution for maintaining the temperature of the structure below 700°C.

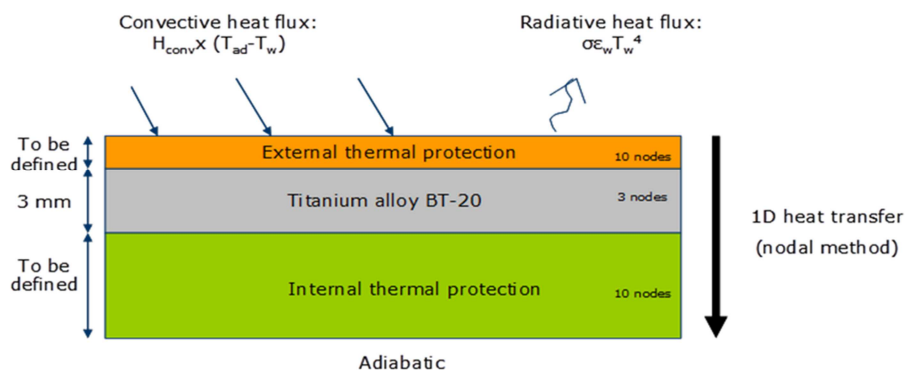


**Fig 3.** Preliminary nodal thermal model of fuselage panel

Analytical local inclination methods (tangent cone method) are used to determine the inviscid flow outside the boundary layer. Wall friction is then calculated thanks to classical analytical correlations valuable for an incompressible flow over a flat plate without pressure gradient. Compressible effects are taken into account thanks to the Eckert reference enthalpy and curvature effects are taken into account thanks to the Mangler transformation. Convective heat flux is finally derived from wall friction using the Reynolds analogy. Gas is considered as a chemically frozen ideal gas (i.e. specific thermal capacity is dependent from temperature) during all the calculation process.

The assumptions of the simulations were:

- $t_{init}=139$  s (fairing release) with  $T_{init}=300$  K ( 27°C)
- Margins on heat fluxes: 1.2 on laminar flow, 1 on turbulent flow
- Laminar to turbulent transition on the complete vehicle:  $t=300.52$  s

The assessed solutions for the external Thermal Protection System (TPS) were: (i) heat sink by increasing the titanium thickness (ii) Prosial ® coating (iii) zirconium coating (iv) high emissivity black paint ( $\epsilon > 0.8$ ).

Despite its high insulating performance, Prosial ® coating used on European launchers was quickly abandoned due to some issues for keeping the aerodynamic shape and due to the high thickness needed for maintaining a low temperature at the interface between the coating and the fuselage.

A parametric approach was used for determining the best solution for the TPS. Table 1 and Table 2 present the maximal temperature (°C) obtained respectively on the windside and leeward fuselage panels for different combinations of TPS.

		Windside fuselage panel					
		Bay 01	Bay 12	Bay 23	Bay 34	Bay 45	Bay 56
Titanium 3 mm	$\epsilon=0.25$	787	762	744	731	721	614
	$\epsilon=0.8$	672	651	636	623	615	523
Titanium 4 mm	$\epsilon=0.25$	730	705	688	674	665	559
	$\epsilon=0.8$	634	612	598	585	577	484
Titanium 3 mm + Zirconia 1 mm	$\epsilon(T)$	671	646	630	616	606	502
	$\epsilon=0.8$	623	601	587	575	566	474
Titanium 5 mm	$\epsilon=0.25$	683	658	642	628	619	515
	$\epsilon=0.8$	601	579	564	552	543	451
Titanium 3 mm + Zirconia 2mm	$\epsilon(T)$	619	595	578	565	556	456
	$\epsilon=0.8$	580	559	544	533	524	435

**Table 1.** Maximal temperature (°C) on the windside fuselage panel of each cargo bay

		Leeward fuselage panel					
		Bay 01	Bay 12	Bay 23	Bay 34	Bay 45	Bay 56
Titanium 1 mm	$\epsilon=0.25$	824	805	791	780	772	765
	$\epsilon=0.8$	669	652	641	631	625	619
Titanium 2 mm	$\epsilon=0.25$	727	707	693	682	674	667
	$\epsilon=0.8$	611	594	581	572	565	558
Titanium 3 mm	$\epsilon=0.25$	656	636	622	611	603	595
	$\epsilon=0.8$	564	546	534	524	517	510
Titanium 4 mm	$\epsilon=0.25$	601	581	567	556	548	541
	$\epsilon=0.8$	524	506	494	484	476	470
Titanium 3 mm + Zirconia 1 mm	$\epsilon(T)$	545	525	512	501	493	486
	$\epsilon=0.8$	514	496	484	474	467	461

**Table 2.** Maximal temperature (°C) on the leeward fuselage panel of each cargo bay

The heat sink method by increasing the titanium thickness was found as a possible solution but it lead to a prohibitive increase of total mass.

Zirconia coating was not found as an interesting solution because its thermal effect was mainly a heat sink effect rather than an insulating effect. It is barely more interesting than increasing titanium thickness whereas its density is higher. This solution was abandoned except for protecting locally some critical points (see section 3.2).

A high emissivity paint ( $\epsilon > 0.8$ ) was found as a sufficient solution for maintaining the temperature of the fuselage panels below 700°C. It is even possible to reduce the thickness of the leeside panels.

Some wind tunnel tests of different paintings are currently on hold in TsAGI premises for verifying the adhesion of those paints at very high speeds.

### 3.2. Detailed FEM simulations

Apart from the main titanium structure of the vehicle, nose, wing leading edges, elevons are the parts submitted to the highest heat fluxes along the trajectory and so they need a dedicated thermal management. Many thermal analyses relying on CFD-FEM based analyses [6] have been performed by CIRA in order to assess different classes of materials: BT-20 titanium alloy, copper, tungsten, C/C-SiC + use of zirconia coating or high emissivity painting as TPS if needed [7].

Due to the fundamental role of the nose, particular attention has been paid to evaluate at early stage the thermal response of this component. Therefore, a detailed feasibility analysis to select the proper material to be employed for the nose manufacturing has been performed considering the hottest portion of a preliminary trajectory ( $\Delta t = 80s$ ). BT-20 titanium alloy, copper and tungsten have been assessed (full C/C-SiC was not considered due to costs reasons).

Fig 4 reports this comparison in terms of temperature contours at the final time step, while Fig 5 shows the time variation of the maximum temperature for the different analysed materials.

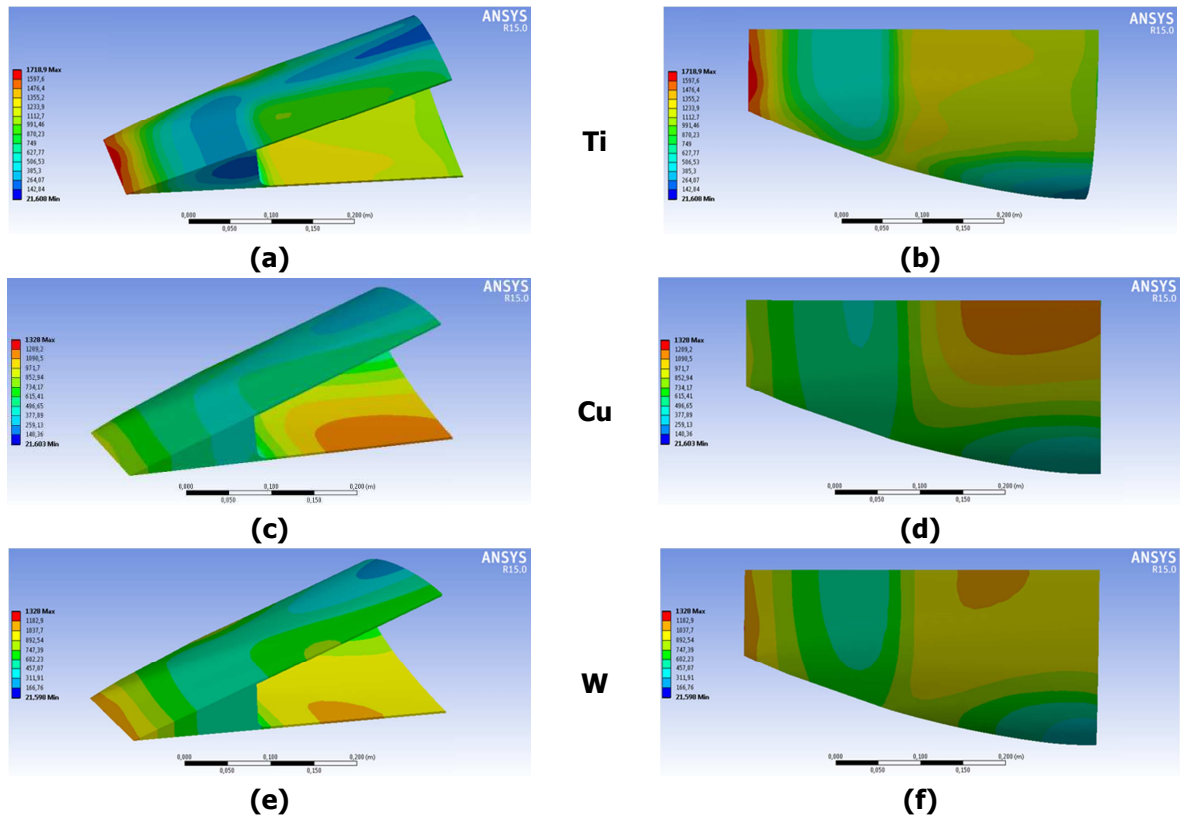


**Fig 4.** Comparison among the temperature distributions inside the nose at the final time step for the different considered materials: titanium (a) and (b) ; copper (c) and (d) ; tungsten (e) and (f)

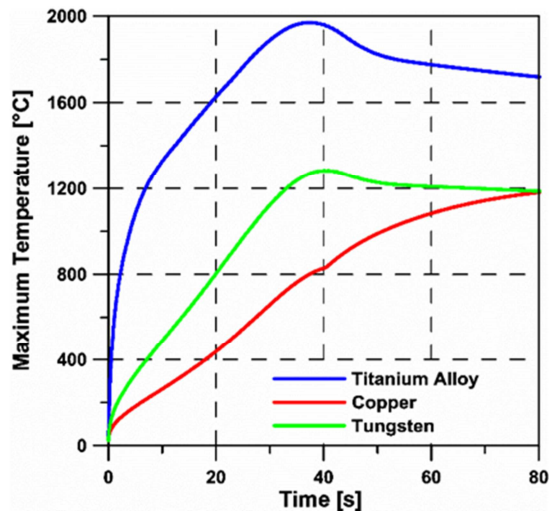


**Fig 5.** Time variation of the maximum temperature on the nose for the different analysed materials

From the previous figures, it is clear that copper is the most suitable material to be employed as a metallic heat sink for the nose, thanks to its high thermal diffusivity. On the other hand, it has not relevant mechanical properties, in particular at high temperatures. For this reason it has to be underlined that the thermal response for copper nose has been optimized properly sizing the material thickness in the aft windside part of the analysed nose cap.

Finally, the preliminary choice of materials for the different components of the vehicle was defined as follows: main structure: BT-20 titanium alloy, nose: copper, wing leading edges & elevons: C/C-SiC. 1 mm thick zirconium coating was also preliminary defined as TPS all over the vehicle.

Nevertheless, one important issue was still the junction of the wing leading edges and the fuselage at the first bay of the vehicle. Actually, due to manufacturing and assembling reasons, it was not possible to use C/C-SiC for such a small leading edge at this junction. Like the nose, it was decided to use copper for the lateral part of the first bay which includes the leading edge. Titanium was still used for the windside and leeside parts of the first bay.

The preliminary choice of materials is finally described in Fig 6:

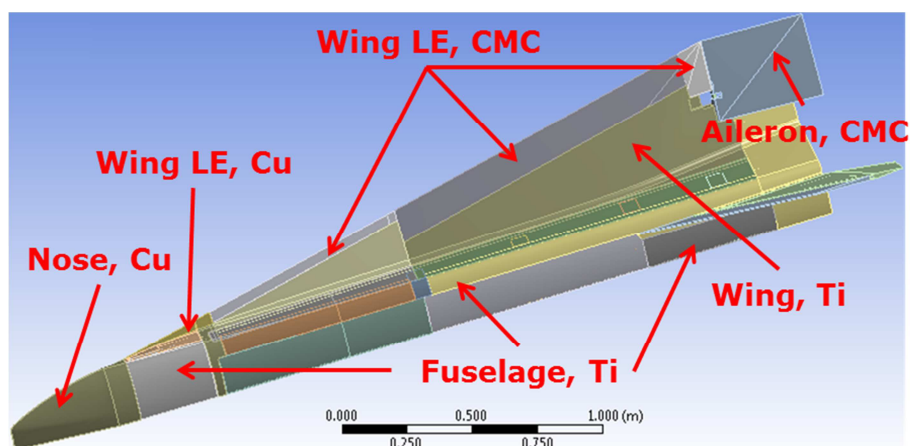
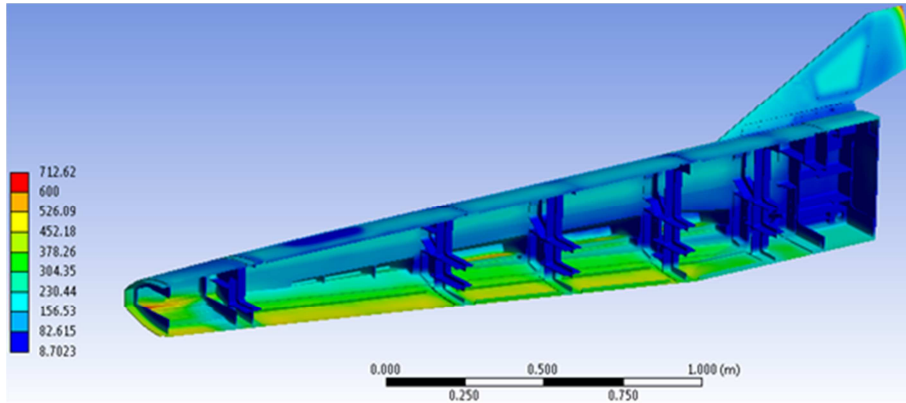


**Fig 6.** Preliminary choice of materials for the different elements of the vehicle

Then, CIRA performed 3D FEM thermal simulations of the complete vehicle along the conservative reference trajectory with this choice of materials and 1 mm thick zirconia coating.

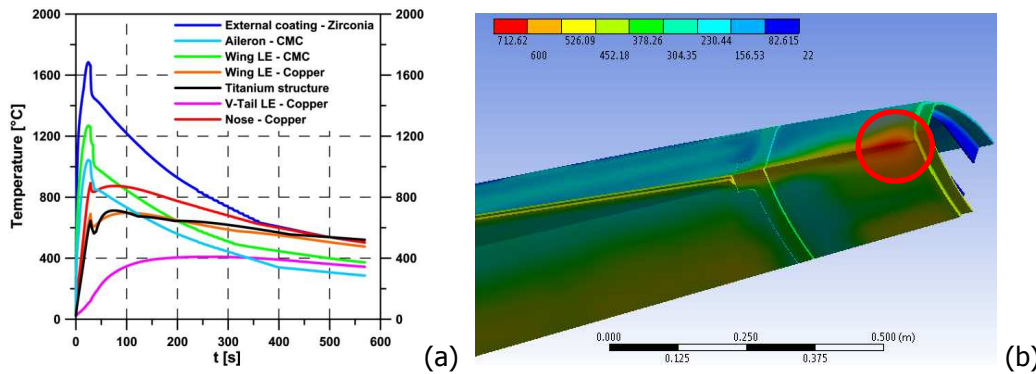
Heating of the internal titanium structure along the trajectory was assessed. **Erreur ! Source du renvoi introuvable.** shows the maximum temperature distribution obtained for the frames and they were found not too hot so that internal equipment could be fixed directly on them (see next section to the thermal management of equipment).





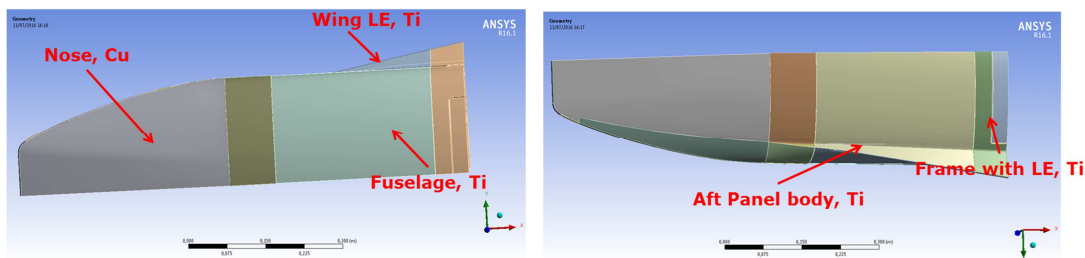
**Fig 7.** Maximal temperature distribution on the titanium internal structure

Fig 8 reports the maximum temperature variations on the main vehicle components. Zirconia coatings and C/C-SiC components would widely survive the aerothermal environment due to their maximum service temperatures of nearly 2400°C and 1600°C respectively. On the other hand, the maximum temperatures on the titanium and copper structures slightly exceed their upper working temperature limits (700°C and 800°C) due to the limited critical area at the junction between the titanium fuselage and the copper leading edge at the first bay.



**Fig 8.** (a) Maximum temperature along the flight profile on the main vehicle components  
(b) Peak heating temperature on the critical area of the wing leading edge

The junction between the fuselage and the leading edge at the first bay was still remaining the main issue. Furthermore, due to assembling and mechanical strength reasons, it was imposed to replace copper with titanium for the entire first bay of the vehicle (see Fig 9).



**Fig 9.** Update of materials for the first bay

Simulations were updated for assessing this new configuration for the first bay. Fig 10 shows the maximal temperatures obtained for a configuration with 1 mm thick zirconium coating. Red color represents all the temperature above 600°C (a), 700°C (b) and 800°C (c). It is clear that even if titanium maximum service temperature would be 800°C, the leading edge area would be still critical and either copper or CMC would be more suitable.



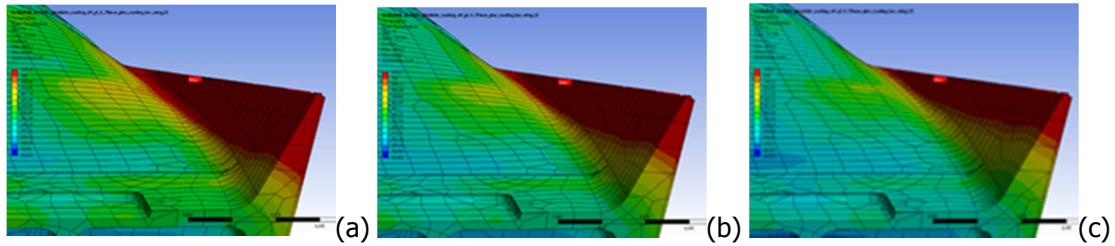
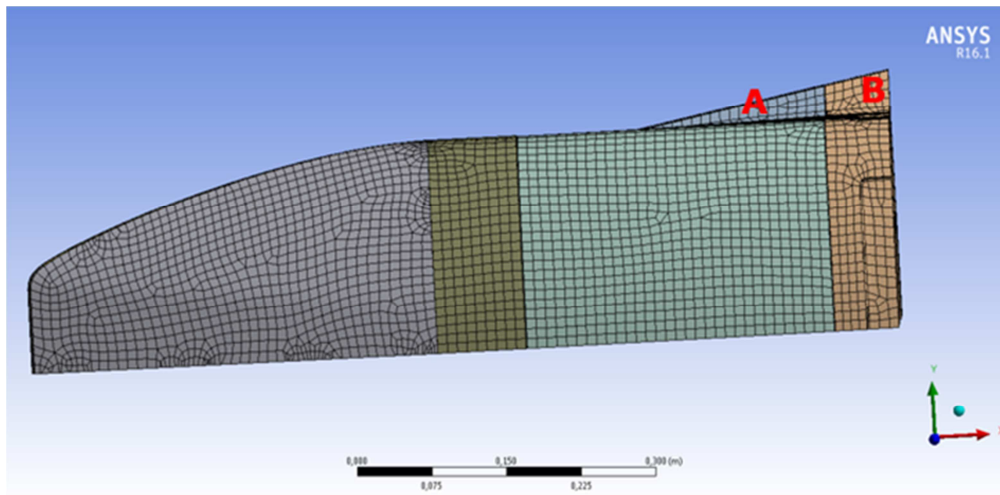


**Fig 10.** Thermal contour- red above 600°C (a), 700°C (b), 800°C (c),

Another design solution has also been suggested. This would take into account the possibility to use a high emissivity paint either directly on spare metals (titanium, copper) or on zirconia coating. This paint would be high-temperature resistant and would guarantee a minimum global emissivity of 0.8.

Several combinations were tested for the first bay and the first frame which connects it to the rest of the vehicle. Table 3 summarizes the maximal temperature obtained on parts A and B for the different combinations.



Material		Tmax (°C)	
A	B	A	B
Cu + 1 mm ZrO <sub>2</sub> everywhere	Ti + 1 mm ZrO <sub>2</sub> everywhere	556	840
Ti + 1 mm ZrO <sub>2</sub> on leading edge	Ti + 1 mm ZrO <sub>2</sub> on leading edge	1200	1230
Ti + 1 mm ZrO <sub>2</sub> on leading edge and wing leeside	Ti + 1 mm ZrO <sub>2</sub> on leading edge and wing leeside	1140	1166
Ti + 1 mm ZrO <sub>2</sub> everywhere (ε=0.8)	Ti + 1 mm ZrO <sub>2</sub> everywhere (ε=0.8)	1010	1033
Ti + 2 mm ZrO <sub>2</sub> everywhere (ε=0.8)	Ti + 2 mm ZrO <sub>2</sub> everywhere (ε=0.8)	878	898

**Table 3.** Material combinations for the first bay and the first frame

Therefore, the most suitable solution that has been taken is to manufacture the so-called B part in CMC and to have for the so-called A part, a full titanium coated by 2 mm of zirconia tailoring to 0 mm moving towards the main structure of the fuselage on the leeside painted with the high emissivity paint.

Finally, a conservative reference trajectory was defined for the thermal analysis and the assumptions of the simulations were:

- $t_{init}=139$  s (fairing release) with  $T_{init}=300$  K ( 27°C)
- Convective boundary condition: CFD computations (several points along the trajectory)
- Laminar to turbulent transition on the complete vehicle:  $t_{transition}=300.52$  s
- Margins on heat fluxes: 1.2 on laminar flow, 1.0 on turbulent flow
- Emissivity values:  $\epsilon_{Ti}=0.25$ ,  $\epsilon_{Cu}=0.14$ ,  $\epsilon_{C/C-SiC}=0.8$ ,  $\epsilon_{ZrO_2}=0.4$

- Max temperatures: Ti (700°C), Cu (800°C), C/C-SiC (1600°C), ZrO<sub>2</sub> (2400°C)

Assuming a high emissivity paint ( $\epsilon > 0.8$ ) applied even on the metallic part and the zirconia coating, the following external TPS is proposed to protect the components of the vehicle:

- Main structure: Titanium without zirconia coating
- Nose: Copper coated by 1 mm of zirconia on the leading edge and windside, tailoring to 0 mm before mechanical connections with the main structure of the fuselage
- Critical area of the wing leading edge (junction with the nose): Titanium coated by 2 mm of zirconia tailoring to 0 mm moving towards the main structure of the fuselage on the leeside
- Elevons and wing leading edges: C/C-SiC

#### 4. Internal equipment

Active cooling could only be used during pre-flight operations (see section 2) for the Thermal Control System (TCS) of the internal equipment. So, different types of passive or semi-passive light solutions were defined depending of the different types of heating modes during the flight:

- Radiative heating: A light internal thermal protection placed on the internal face of the fuselage panels should be thick enough so that radiative heating could be neglected. This thermal protection could also wrap the equipment but it would prevent them from dissipating their own heating by Joule effect during pre-flight and flight.
- Conductive heating: The heat sink effect of the internal frames and the moderate thermal conductivity of titanium are used for keeping the fixation points of the equipment at a moderate temperature. If necessary, bolts, nuts, could be based on an insulating material for reducing conductive heating.
- Joule effect heating: A high emissivity painting could be applied on the equipment so as to promote its heat dissipation. If not efficient enough, a heat sink could be introduced between the equipment and the internal frame so as to dissipate additional energy into the sink.
- Free convective heating: As pressure into the vehicle is very low at high altitudes, this heating mode could be neglected during the mission

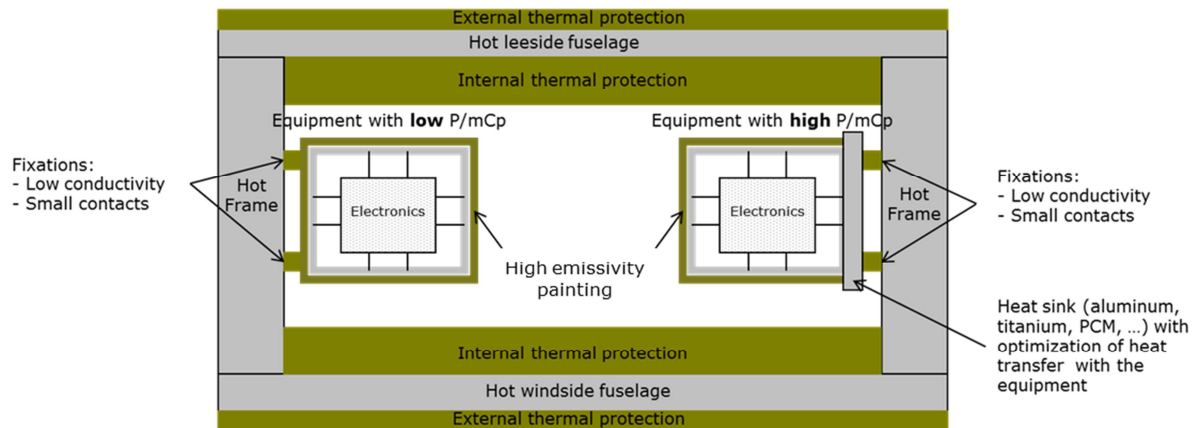


**Fig 11.** Thermal Control System of the internal equipment

##### 4.1. Radiative heating during flight

The main source of equipment heating is the thermal radiation coming from the panels of the structure. ONERA and ESA designed an internal thermal protection system based on a light flexible microporous insulator named Aeroguard® provided by PROMAT firm in Belgium. This material is able to withstand 1000°C and it exhibits an extra low thermal conductivity at sea pressure which could be even largely reduced at low pressure at high altitude.



**Technical data**

Brand	AEROGUARD®					
	128	160	190	220		
Density	kg/m³	128	160	190	220	
Textile covering		SD - ED - HD				
Stitching pitch size		25x25mm				
Classification temperature	°C	1000	1000	1000	1000	
Compressive strength (ASTM C 165)	MPa = N/mm²	0.04	0.05	0.07	0.10	
Thermal conductivity (ISO 8302, ASTM C177)	200°C mean	W/m.K	0.029	0.031	0.030	0.027
	400°C mean	W/m.K	0.043	0.040	0.037	0.031
	600°C mean	W/m.K	0.066	0.051	0.047	0.039
	800°C mean	W/m.K	0.098	0.064	0.060	0.050
Specific heat capacity	200°C	kJ/kg.K	0.92	0.92	0.92	0.92
	400°C	kJ/kg.K	1.00	1.00	1.00	1.00
	600°C	kJ/kg.K	1.04	1.04	1.04	1.04
	800°C	kJ/kg.K	1.08	1.08	1.08	1.08
Shrinkage	1-sided 12h @1000°C	%	< 0.5	< 0.5	< 0.5	< 0.5
	Full soak 24h @1000°C	%	< 3	< 3	< 3	< 3

**Fig 12.** Aeroguard® internal thermal protection system

ONERA performed 1D thermal simulations (see section 3.1) by taking into account depressurization effect into the stratosphere. Fig 13 presents the time evolution of the temperature of the inner face of the thermal protection for different thicknesses of Aeroguard 160 ® placed on the windside of the second cargo bay. A thickness of 18 mm was found enough for not heating the equipment.

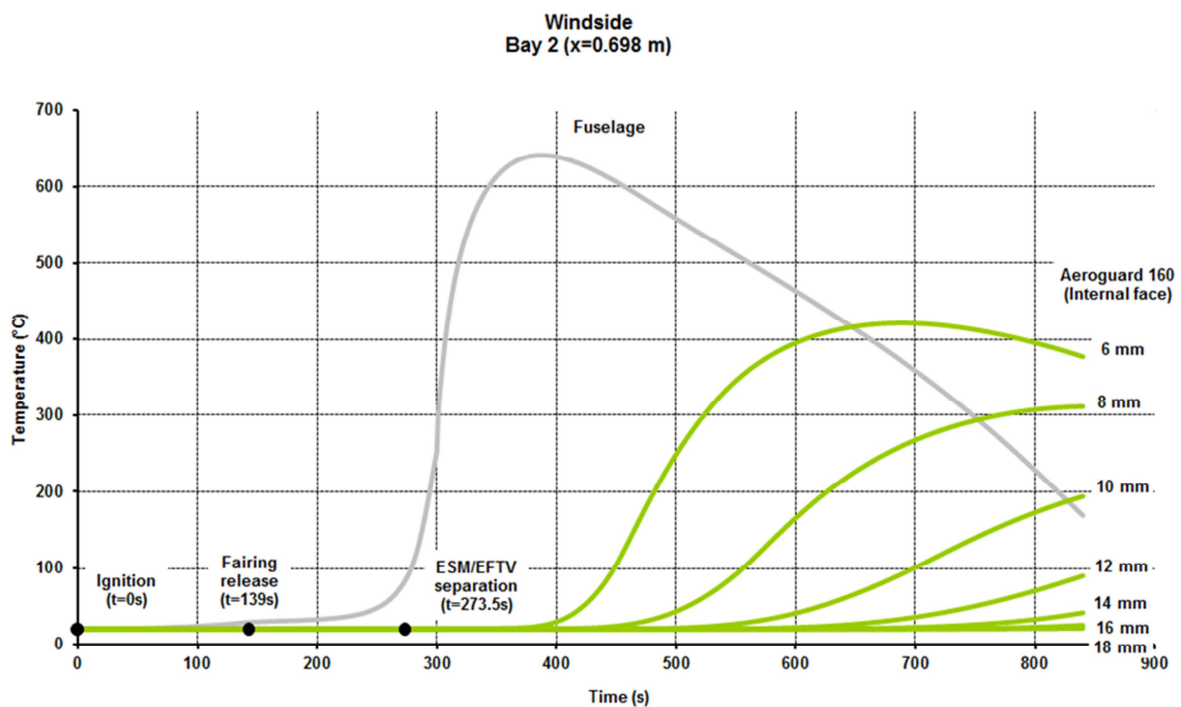


**Fig 13.:** Temperature of the internal thermal protection (inner face) for different thicknesses

Therefore, the thermal control system is composed of two layers of 9 mm thick Aeroguard 160 ® panels which are kept in place with respect to the structure thanks to only thin wires fixed at their extremities to the internal frames of the structure. This smart fixation allows fast depressurization of the insulation panels and optimization of the mass while withstanding mechanical vibrations during the boosted phase of the flight.

To protect the actuators, it was not possible to place the thermal protection on the fuselage so as to allow experiments which aim to detect the laminar to turbulent transition thanks to infrared cameras. A jacket based on the same material was designed for enveloping each actuator and its associated actuation line (see [9]).



**Fig 14.** Aeroguard 160 ® based jacket of the actuators

Thermal tests are currently taking place at the Von Karman Institute in order to verify the thermal behaviour of the stack during depressurization.

#### 4.2. Conductive heating during flight

Almost all equipment is fixed on the internal frames of the main structure. So as to slow conductive heat transfer coming from the structure, nuts and bolts of the fixations are based on the low thermal conductivity ( $\approx 0.29 \text{ W/m/K}$ ) Vespel® material able to withstand  $260^\circ\text{C}$  in continuous operation.



**Fig 15.** Vespel® bolt and washer

#### 4.3. Joule effect heating during pre-flight and flight

Internal equipment is switched on nearly 20 min before the booster ignition. During these pre-flight operations and then during all the flight, equipment is heated up because of its own Joule effect. This energy is poorly evacuated into the internal structure due to the insulating bolts, washers, nuts at the fixation points (see previous section) and free convection is also very limited due to the low pressure into the vehicle at high altitudes.

So, a high emissivity paint is recommended for dissipating the energy. If not efficient enough, a metallic heat sink could be introduced between the equipment and the fixation frame.

ONERA performed OD nodal thermal simulations of the equipment alone. A high emissivity paint is sufficient to dissipate the heat for most of equipment except for telemetry boxes. Sizing of an adequate aluminum heat sink leads to a prohibitive increase of mass and occupied volume.

A light and compact solution consists in using a rectangular aluminum box containing phase changing material. These boxes are designed by WALOPT firm and manufactured by CRM in Belgium [8].

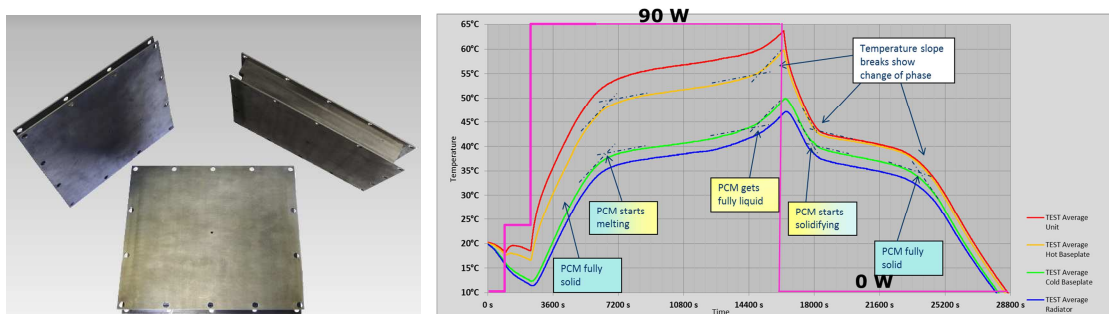


**Fig 16.** Phase Changing Material (PCM) heat sink plate

## Acknowledgements

This work was performed within the 'High Speed Experimental Fly Vehicles - International' project fostering International Cooperation on Civil High-Speed Air Transport Research. HEXAFLY-INT, coordinated by ESA-ESTEC, is supported by the EU within the 7th Framework Programme Theme 7 Transport, Contract no.: ACP3-GA-2014-620327 and by the Ministry of Industry and Trade, Russian Federation. Further info on HEXAFLY-INT project can be found on [http://www.esa.int/techresources/hexafly\\_int](http://www.esa.int/techresources/hexafly_int).

## References

- [1] Steelant J., 'Achievements Obtained for Sustained Hypersonic Flight within the LAPCAT Project', 15th AIAA International Space Planes and Hypersonic Systems and Technologies Conference, AIAA-2008-2578, 28 April- 01 May 2008, Dayton, Ohio, USA.
- [2] Steelant, J., Varvill R., Defoort S., Hannemann K. and Marini M., 'Achievements Obtained for Sustained Hypersonic Flight within the LAPCAT-II Project', 20th AIAA International Space Planes and Hypersonic Systems and Technologies Conference, AIAA-2015-3677, 5-8 July 2015, Glasgow, Scotland.
- [3] Steelant J., 'ATLLAS: Aero-Thermal Loaded Material Investigations for High-Speed Vehicles', 15th AIAA International Space Planes and Hypersonic Systems and Technologies Conference, AIAA-2008-2582, 28 April-01 May 2008, Dayton, Ohio, USA.
- [4] Steelant J., Dalenbring M. ., Kuhn M., Bouchez M. and von Wolfersdorf J., 'Achievements obtained within the ATLLAS-II Project on Aero-Thermal Loaded Material Investigations for High-Speed Vehicles', 21st Int. Space Planes and Hypersonic Systems and Technology Conference, AIAA-2017-2393, 6-9 March 2017, Xiamen, China.
- [5] Steelant J., Langener T., Hannemann K., Riehmer J., Kuhn M., Dittert C., Jung W., Marini M., Pezzella G., Cicala M. and Serre L., 'Conceptual Design of the High-Speed Propelled Experimental Flight Test Vehicle HEXAFLY', 20th AIAA International Space Planes and Hypersonic Systems and Technologies Conference, AIAA-2015-3539, 5-8 July 2015, Glasgow, Scotland.
- [6] Scigliano R. , Pezzella G., Di Benedetto S., Marini M. and Steelant J., "HEXAFLY-INT Experimental Flight Test Vehicle (EFTV) Aero-Thermal Design", ASME International Mechanical Engineering Congress & Exposition (IMECE), IMECE2017-70392, 3-9 November 2017, Tampa, Florida, USA.
- [7] Roberto Scigliano, Valerio Carandente, Design Analysis of The HEXAFLY-Int Thermal Protection System, 8th European Workshop on TPS & Hot Structures, 19-22 April 2016, ESA/ESTEC, Noordwijk, The Netherlands.
- [8] Peyrou-Lauga R., Collette J.-P. and Nutal N., 'Phase Change Material Heat Storage Device for Launchers and Orbiting Systems', 45<sup>th</sup> International Conference on Environmental Systems 12-16 July 2015, Bellevue, Washington, ICES-2015-231
- [9] Andro J.-Y., Rotärmel W., Nebula F., Morani G. and Steelant J., Design of the Actuation System of the Hexafly-int Hypersonic Glider, International Conference on High Speed Vehicle Science and Technology (HiSST), November 26<sup>th</sup> – 29<sup>th</sup> 2018, Moscow, Russia